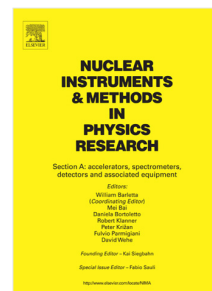


## Accepted Manuscript

HERMES: An ultra-wide band X and gamma-ray transient monitor on board a nano-satellite constellation

F. Fuschino, R. Campana, C. Labanti, Y. Evangelista, M. Feroci, L. Burderi, F. Fiore, F. Ambrosino, G. Baldazzi, P. Bellutti, R. Bertacin, G. Bertuccio, G. Borghi, D. Cirrincione, D. Cauz, F. Ficorella, M. Fiorini, M. Gandola, M. Grassi, A. Guzman, G. La Rosa, M. Lavagna, P. Lunghi, P. Malcovati, G. Morgante, B. Negri, G. Pauletta, R. Piazzolla, A. Picciotto, S. Pirrotta, S. Pliego-Caballero, S. Puccetti, A. Rachevski, I. Rashevskaya, L. Rignanese, M. Salatti, A. Santangelo, S. Silvestrini, G. Sottile, C. Tenzer, A. Vacchi, G. Zampa, N. Zampa, N. Zorzi



PII: S0168-9002(18)31681-4  
DOI: <https://doi.org/10.1016/j.nima.2018.11.072>  
Reference: NIMA 61613

To appear in: *Nuclear Inst. and Methods in Physics Research, A*

Received date: 3 July 2018  
Revised date: 9 November 2018  
Accepted date: 13 November 2018

Please cite this article as: F. Fuschino, R. Campana, C. Labanti et al., HERMES: An ultra-wide band X and gamma-ray transient monitor on board a nano-satellite constellation, *Nuclear Inst. and Methods in Physics Research, A* (2018), <https://doi.org/10.1016/j.nima.2018.11.072>

This is a PDF file of an unedited manuscript that has been accepted for publication. As a service to our customers we are providing this early version of the manuscript. The manuscript will undergo copyediting, typesetting, and review of the resulting proof before it is published in its final form. Please note that during the production process errors may be discovered which could affect the content, and all legal disclaimers that apply to the journal pertain.

---

1 NIMA POST-PROCESS BANNER TO BE  
2 REMOVED AFTER FINAL ACCEPTANCE

---

3 HERMES: An ultra-wide band X and gamma-ray  
4 transient monitor on board a nano-satellite  
5 constellation

6 F. Fuschino<sup>a,b,\*</sup>, R. Campana<sup>a,b</sup>, C. Labarini<sup>a,b</sup>, Y. Evangelista<sup>c,d</sup>, M. Feroci<sup>c,d</sup>,  
7 L. Burderi<sup>e</sup>, F. Fiore<sup>h</sup>, F. Ambrosini<sup>o</sup>, G. Baldazzi<sup>e,b</sup>, P. Bellutti<sup>q</sup>,  
8 R. Bertacin<sup>r</sup>, G. Bertuccio<sup>m,n</sup>, C. Longini<sup>q</sup>, D. Cirrincione<sup>i,k</sup>, D. Cauzi<sup>i,j</sup>,  
9 F. Ficorella<sup>q</sup>, M. Fiorini<sup>f</sup>, M. Gardola<sup>m,n</sup>, M. Grassi<sup>o</sup>, A. Guzman<sup>t</sup>,  
10 G. La Rosa<sup>s</sup>, M. Lavagna<sup>p</sup>, P. Lunghi<sup>p</sup>, P. Malcovati<sup>o</sup>, G. Morgante<sup>a</sup>,  
11 B. Negri<sup>r</sup>, G. Pauletta<sup>j</sup>, R. Piazzolla<sup>c</sup>, A. Picciotto<sup>q</sup>, S. Pirrotta<sup>r</sup>,  
12 S. Pliego-Caballero<sup>t</sup>, S. Puccetti<sup>r</sup>, A. Rachevski<sup>k</sup>, I. Rashevskaya<sup>l</sup>,  
13 L. Rignanese<sup>e,b</sup>, M. Salatti<sup>r</sup>, L. Santangelo<sup>t</sup>, S. Silvestrini<sup>p</sup>, G. Sottile<sup>s</sup>,  
14 C. Tenzer<sup>t</sup>, A. Vacchi<sup>l</sup>, G. Zampa<sup>k</sup>, N. Zampa<sup>k</sup>, N. Zorzi<sup>q</sup>

15 <sup>a</sup>INAF-CAS Fognanò, Via Gobetti 101, I-40129 Bologna, Italy

16 <sup>b</sup>INFN sez. Bologna, Viale Berti-Pichat 6/2, I-40127 Bologna, Italy

17 <sup>c</sup>INAF-IAPS, Via del Fosso del Cavaliere 100, I-00133 Rome, Italy

18 <sup>d</sup>INFN sez. Roma 2, Via della Ricerca Scientifica 1, I-00133 Rome, Italy

19 <sup>e</sup>University of Bologna, Dep. of Physics and Astronomy - DIFA, viale Berti Pichat 6/2,  
20 I-40127 Bologna, Italy

21 <sup>f</sup>INAF-IASF Milano, Via Bassini 15, I-20100 Milano, Italy

22 <sup>g</sup>University of Cagliari, Dep. of Physics, S.P. Monserrato-Sestu Km 0,700, I-09042  
23 Monserrato (CA), Italy

24 <sup>h</sup>INAF-OATs Via G.B. Tiepolo, 11, I-34143 Trieste

25 <sup>i</sup>University of Udine, Via delle Scienze 206, I-33100 Udine, Italy

26 <sup>j</sup>INFN Udine, Via delle Scienze 206, I-33100 Udine, Italy

27 <sup>k</sup>INFN sez. Trieste, Padriciano 99, I-34127 Trieste, Italy

28 <sup>l</sup>TIFPA-INFN, Via Sommarive 14, I-38123 Trento, Italy

29 <sup>m</sup>Politecnico di Milano, Department of Electronics, Information and Bioengineering, Via  
30 Anzani 42, I-22100 Como, Italy

31 <sup>n</sup>INFN sez. Milano, Via Celoria 16, I-20133 Milano, Italy

32 <sup>o</sup>University of Pavia, Department of Electrical, Computer, and Biomedical Engineering,  
33 and INFN Sez. Pavia, Via Ferrata 3, I-27100 Pavia, Italy

34 <sup>p</sup>Politecnico di Milano, Bovisa Campus, Via La Masa 34 - I-20156 Milano, Italy

---

\*Corresponding author

Email address: [fuschino@iasfbo.inaf.it](mailto:fuschino@iasfbo.inaf.it) (F. Fuschino)

35 <sup>a</sup>Fondazione Bruno Kessler – FBK, Via Sommarive 18, I-38123 Trento, Italy  
36 <sup>r</sup>Italian Space Agency - ASI, Via del Politecnico snc, 00133 Roma, Italy  
37 <sup>s</sup>INAF/IASF Palermo, Via Ugo La Malfa 153, I-90146 Palermo, Italy  
38 <sup>t</sup>University of Tübingen-IAAT, Sand 1, D-72076 Tübingen, Germany

---

39 **Abstract**

The High Energy Modular Ensemble of Satellites (HERMES) project is aimed to realize a modular X/gamma-ray monitor for transient events, to be placed on-board of a nano-satellite bus (e.g. CubeSat). This expandable platform will achieve a significant impact on Gamma-Ray Burst (GRB) science and on the detection of Gravitational Wave (GW) electromagnetic counterparts: the recent LIGO/VIRGO discoveries demonstrated that the high-energy transient sky is still a field of extreme interest. The very complex temporal variability of GRBs (experimentally verified up to the millisecond scale) combined with the spatial and temporal coincidence between GWs and their electromagnetic counterparts suggest that upcoming instruments require sub-microsecond time resolution combined with transient localization accuracy lower than a degree. The current phase of the ongoing HERMES project is focused on the realization of a technological Pathfinder with a small network (3 units) of nano-satellites to be launched in mid 2020. We will show the potential and prospects for short and medium-term development of the project, demonstrating the disrupting possibilities for scientific investigations provided by the innovative concept of a new “modular astronomy” with nano-satellites (e.g. low developing costs, very short realization time). Finally, we will illustrate the characteristics of the HERMES Technological Pathfinder project, demonstrating how the scientific goals discussed are actually already reachable with the first nano-satellites of this constellation. The detector architecture will be described in detail, showing that the new generation of scintillators (e.g. GAGG:Ce) coupled with very performing Silicon Drift Detectors (SDD) and low noise Front-End-Electronics (FEE) are able to extend down to few keV the sensitivity band of the detector. The technical solutions for FEE, Back-End-Electronics (BEE) and Data

Handling will be also described.

40 *Keywords:* Nanosatellites, Gamma-ray Burst, Silicon Drift Detectors,  
41 Scintillator Detectors  
42 *PACS:* 95.55.Ka, 29.40.Wk, 29.40.Mc,

---

### 43 1. Introduction

44 Gamma-Ray Bursts (GRBs) are one of the most intriguing and challeng-  
45 ing phenomena for modern science. Their study is of very high interest for  
46 several fields of astrophysics, such as the physics of matter in extreme condi-  
47 tions and black holes, cosmology, fundamental physics and the mechanisms of  
48 gravitational wave signal production, because of their huge luminosities, up to  
49 more than  $10^{52}$  erg/s, their red-shift distribution extending from  $z \sim 0.01$  up to  
50  $z > 9$  (i.e., much above that of supernovae of the Ia class and galaxy clusters),  
51 and their association with peculiar core-collapse supernovae and with neutron  
52 star/black hole mergers.

53 Since their discovery, GRBs were promptly identified as having a non-terrestrial  
54 origin [1]. First observations were done using radiation monitors onboard the  
55 VELA spacecraft constellation, that was a network of satellites designed to mon-  
56 itor atmospheric nuclear tests. Between 1963 and 1970 a total of 12 satellites  
57 were launched and the constellation was operating until 1985, with more sen-  
58 sitive detectors on later satellites. By analyzing the different arrival times of  
59 the  $\gamma$ -ray photon bursts as detected by different satellites, placed in different  
60 locations around the Earth, it was possible to roughly estimate the direction  
61 of the GRB, later improved using additional and better detectors, reaching a  
62 precision of  $\sim 10^\circ$ . With a very similar approach, the Inter-Planetary Network  
63 (IPN<sup>1</sup>, including all satellites with GRB-sensitive instruments on-board) was  
64 organised by GRB scientists in late '70s, aiming to localize GRBs for the ob-  
servation of counterparts at other wavelengths. Basing on the availability of

---

<sup>1</sup><https://heasarc.gsfc.nasa.gov/w3browse/all/ipngrb.html>

66 operating instruments, the IPN in its lifetime has involved up to more than 20  
67 different spacecrafts. This experience demonstrates that the localization accu-  
68 racy of GRBs is improved by increasing the spacing between different detectors,  
69 and also by a more accurate detector timing resolution. The IPN localizations  
70 are usually provided in few days, and although can reach angular resolutions of  
71 arcminutes and often arcseconds, the current typical accuracy, at high energies,  
72 is of the order of few degrees. This was demonstrated, e.g., in the case of the  
73 discovery of Gravitational Wave (GW) electromagnetic counterparts [2]. Such  
74 huge error box is too large to be efficiently surveyed at optical wavelengths,  
75 where tens/hundreds of optical transient sources are usually found, increasing  
76 enormously the probability to find spurious correlations. The best strategy here  
77 is to perform a prompt search for transients at high energies, with a localiza-  
78 tion accuracy of arcminutes or arcseconds, reducing the probability of chance  
79 association.

## 80 2. HERMES Mission Concept

81 The *High Energy Modular Ensemble of Satellites* (HERMES) project aims  
82 to realize a new generation instrument for the observations of high-energy tran-  
83 sients. The proposed approach here differs from the conventional idea to build  
84 increasingly larger and expensive instruments. The basic HERMES philosophy  
85 is to realize innovative, distributed and modular instruments composed by  
86 tens/hundreds of simple units, cheaper and with a limited development time.  
87 The present nanosatellite (e.g. CubeSats) technologies demonstrates that off-  
88 the-shelf components for space use can offer solid readiness at a limited cost.  
89 For scientific applications, the physical dimension of a single detector should to  
90 be compatible with the nanosatellite structure (e.g. 1U CubeSat of  $10\times 10\times 10$   
91 cm<sup>3</sup>). Therefore, the single HERMES detector is of course underperforming  
92 (i.e. it has a low effective area), when compared with conventional operative  
93 transient monitors, but the lower costs and the distributed concept of the in-  
94 strument demonstrate that is feasible to build an innovative instrument with

95 unprecedented sensitivity. The HERMES detector will have a sensitive area  
 96  $>50 \text{ cm}^2$ , therefore with several tens/hundreds of such units a total sensitive  
 97 area of the order of magnitude of  $\sim 1 \text{ m}^2$  can be reached.

98 By measuring the time delay between different satellites, the localisation  
 99 capability of the whole constellation is directly proportional to the number of  
 100 components and inversely proportional to the average baseline between them.  
 101 As a rough example, with a reasonable average baseline of  $\sim 7000 \text{ km}$  (comparable  
 102 to the Earth radius, and a reasonable number for low-Earth satellites in  
 103 suitable orbits) and  $\sim 100$  nanosatellites simultaneously detecting a transient,  
 104 a source localisation accuracy of the order of magnitude of  $\sim 10 \text{ arcsec}^2$  can be  
 105 reached, for transients with short time scale (ms) variability.

106 The current phase of the project, *HERMES Technological Pathfinder* (TP),  
 107 focuses on the realization of three nanosatellites, ready for launch at mid-2020.  
 108 The purpose here is to demonstrate the feasibility of the HERMES concept,  
 109 operating some units in orbit and to detect a few GRBs. The next phase of the  
 110 project, *HERMES Scientific Pathfinder* (SP), will demonstrate the feasibility of  
 111 GRB localisation using up to 6–8 satellites in orbit. Although in both these pre-  
 112 liminary phases reduced ground segment capabilities will be used, i.e. reduced  
 113 data-downloading with a few ground contacts/day, the complete development  
 114 of the HERMES detectors is expected. These activities will pave the way to the  
 115 final HERMES constellation composed of hundreds of nanosatellites. Detailed  
 116 mission studies, including orbital configuration, attitude control strategy, and  
 117 sensitive area distribution will be performed, as well as a proper planning of  
 118 the ground segment allowing to reach the ambitious scientific requirements, i.e.  
 119 prompt diffusion of the transient accurate localization. Thanks to the produc-  
 120 tion approach, the context of a typical Small or Medium-class space mission  
 121 seems to be compatible with HERMES final constellation, where most of the  
 122 resources will be devoted to the multiple launches and to the realization of the

---

$2\sigma_{\text{pos}} = \sigma_{\text{CCF}}/Bc\sqrt{N(N-1-2)} \approx 10 \text{ arcsec}$ ; where  $B$  is the baseline,  $N$  the number of  
 satellites and  $\sigma_{\text{CCF}}$  is the error associated with the cross-correlation function.

123 ground segment.

### 124 **3. Payload Description**

125 A possible solution for the HERMES payload is allocated in 1U-Cubesat  
126 ( $10 \times 10 \times 10$  cm<sup>3</sup>), cf. Figure 1. A mechanical support is placed on the in-  
127 strument topside. The support is composed by two parts to accommodate an  
128 optical/thermal filter in the middle. The electronic boards for the Back-End  
129 and the Data Handling unit are allocated on the bottom of the payload unit.  
130 The detector core is located in the middle: this is a scintillator-based detector  
131 in which Silicon Drift Detectors (SDD, [5]) are used to both detect soft X-rays  
132 (by direct absorption in silicon) and to simultaneously readout the scintillation  
133 light. The payload unit is expected to allocate a detector with  $>50$  cm<sup>2</sup> sen-  
134 sitive area in the energy range from  $3-5$  keV up to 2 MeV, with a total power  
135 consumption  $<4$  W and total weight of  $<1.5$  kg.

#### 136 *3.1. Detector core architecture*

137 Aiming at designing a compact instrument with a very wide sensitivity band,  
138 the detector is based on the so-called “siswich” concept [3, 4], exploiting the  
139 optical coupling of silicon detectors with inorganic scintillators. The detector  
140 is composed by an array of scintillator pixels, optically insulated, read out by  
141 Silicon Drift Detectors.

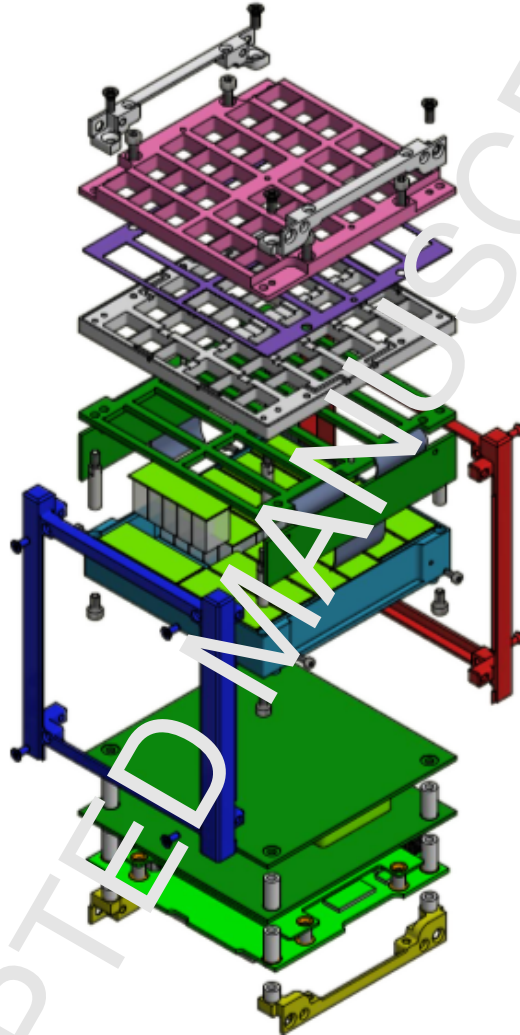


Figure 1: Exploded view of the payload unit ( $10 \times 10 \times 10 \text{ cm}^3$ ) on board the HERMES nanosatellite. From the top are shown the mechanical support composed by top (pink) and bottom (gray) parts, with optical filter (violet) in middle, the FEE board (dark green) allocating SDD matrices (light green), FE-LYRA chips on the top and BE-LYRA chips folded on the side (not shown for clarity), the GAGG crystal pixels (white transparent) and their housing (greenish blue). Mechanical ribs on top (grey) and on bottom (yellow) are also visible, necessary to fix the payload components to the satellite structure (blue and red).

142 In this concept the SDDs play the double role of read-out device for the opti-  
 143 cal signal from the scintillator and of an independent X-ray solid state detector.



144 Low energy X-rays are directly absorbed by the SDD, while higher energy X-  
145 rays and  $\gamma$ -rays are absorbed in the crystal and the optical scintillation photons  
146 are collected by the same detector. Only very low noise readout sensors and  
147 front-end electronics allow to reach a low energy scintillator threshold below  
148 20–30 keV. Above these energies the increasing sensitivity of the scintillator is  
149 able to compensate the lack of efficiency of thin silicon sensors (450  $\mu\text{m}$ ), so  
150 a quite flat efficiency in a wide energy band for the whole integrated system  
151 is reached. The inorganic scintillators selected for this innovative detector is  
152 the recently developed [6] Cerium-doped Gadolinium-Aluminum-Gallium Gar-  
153 net (Ce:GAGG), a very promising material with all the required characteristics,  
154 i.e. a high light output ( $\sim 50,000$  ph/MeV), no internal radioactive background,  
155 no hygroscopicity, a fast radiation decay time of  $\sim 90$  ns, a high density (6.63  
156  $\text{g}/\text{cm}^3$ ), a peak light emission at 520 nm and an effective mean atomic number of  
157 54.4. All these characteristics make this material very suitable for the HERMES  
158 application. Since GAGG is a relatively new material, it has not yet extensively  
159 investigated with respect to radiation resistance and performance after irradi-  
160 ation, although the published results are very encouraging [7–9]. These tests  
161 showed that GAGG has a very good performance, compared to other scintillator  
162 materials largely used in the recent years in space-borne experiments for  $\gamma$ -ray  
163 astronomy (e.g. BGO or CsI), i.e. a very low activation background (down to  
164 2 orders of magnitude lower than BGO), and a minor light output degradation  
165 with accumulated dose.

166 The SDD development builds on the state-of-the-art results achieved within  
167 the framework of the Italian ReDSOX collaboration, with the combined de-  
168 sign and manufacturing technology coming by a strong synergy between INFN-  
169 Trieste and Fondazione Bruno Kessler (FBK, Trento), in which both INFN and  
170 FBK co-fund the production of ReDSOX Silicon sensors. A custom geometry for  
171 a SDD matrix (Figure 2) was designed, in which a single crystal ( $\sim 12.1 \times 6.94$   
172  $\text{cm}^2$ ) is coupled with two SDD channels. Therefore, the scintillator light uni-  
173 formly illuminates two cells, giving rise to a comparable signal output for both  
174 channels. This allows to discriminate scintillator events (higher energy  $\gamma$ -rays)

175 by their multiplicity: lower energy X-rays, directly absorbed in the SDD, are  
 176 read out by only one channel.

### 177 3.2. Readout ASIC: from VEGA to LYRA

178 The HERMES detector, constituted by 120 SDD cells distributed over a total  
 179 area of  $\sim 92 \text{ cm}^2$ , requires a peculiar architecture for the readout electronics.  
 180 A low-noise, low-power Application Specific Integrated Circuit (ASIC) named  
 181 LYRA has been conceived and designed for this task. LYRA has an heritage  
 182 in the VEGA ASIC [10, 11] that was developed by Politecnico of Milano and  
 183 University of Pavia within the ReDSOX Collaboration during the LOFT Phase-  
 184 A study (ESA M3 Cosmic Vision program), although a specific and renewed  
 185 design is necessary to comply with the different SDD specifications, the unique  
 186 system architecture and the high signal dynamic range needed for HERMES. A  
 187 single LYRA ASIC is conceived to operate as a constellation of 32+1 Integrated  
 188 Circuit (IC) chips. The 32 Front-End ICs (FE-LYRA) include preamplifier, first  
 189 shaping stage and signal line-transmitter, the single Back-End IC (BE-LYRA)  
 190 is a 32-input ASIC including all the circuits to complete the signal processing  
 191 chain: signal receiver, second shaping stage, discriminators, peak&hold, control  
 192 logic, configuration registers and multiplexer. The FE-LYRA ICs are small  
 193 ( $0.9 \times 0.6 \text{ mm}^2$  die) allowing to be placed very close to the SDD anodes, in  
 194 order to minimize the stray capacitances of the detector-preamplifier connection,  
 195 maximizing the effective-to-geometric area ratio ( $\sim 54 \text{ cm}^2$  vs.  $\sim 92 \text{ cm}^2$ ). In  
 196 this configuration (Figure 2), the BE-LYRA chips ( $\sim 6.5 \times 2.5 \text{ mm}^2$  die) can be  
 197 placed out of the detection plane, allocating SDD matrix and FE-LYRA ICs  
 198 on a rigid part by means of embedded flex cables. The flat cables allow also  
 199 avoiding the additional space required by connectors, offering the possibility to  
 200 “flip” the boards allocating the BE-LYRA chips (on a rigid part) at right angle  
 201 with respect to the detection plane, on the external side of the payload unit.

### 202 3.3. Back-End Electronics

203 The Back-End electronics (BEE) of HERMES includes the BE-LYRA chips,  
 204 external commercial analog-to-digital (ADC) converters and a FPGA-based con-

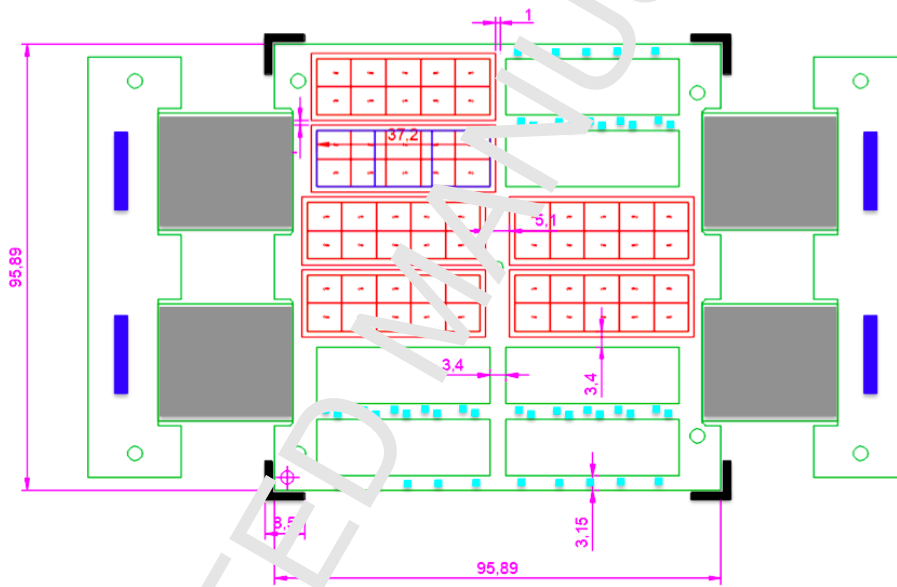


Figure 2: Sketch of the top view of FEE board for the HERMES nanosatellite. The black corner indicate the overall nanosatellite structure ( $10 \times 10 \text{ cm}^2$ ). The board will allocate SDD matrices (in red) and FE-LYRA chips (light blue) very close to each SDD anode. The BE-LYRA chips (blue) are allocated on the rigid part that will be folded on the side of the satellite, by means of flex cables (gray).

205 trol logic. The control logic takes care of the signal handshake required to  
206 read out analogue signals from BE-LYRA chips, synchronizing the digital conver-  
207 sion operations, and time tagging the events based on conventional GPS sensor,  
208 combining an atomic clock signal (CSAC) to reduce as much as possible the  
209 natural shift/jitter of the GPS sensor ensuring a sub-microsecond timing reso-  
210 lution. Due to the peculiar architecture of the detector core, the BEE will also  
211 perform the Event Data Generator functionality: automatically discriminating  
212 the location of photon interaction (silicon or scintillator), on the basis of the  
213 multiplicity of the readout signals. This fundamental task has to be carried  
214 out in real-time to generate the photon lists that include channel address, time  
215 of arrival of photons and a raw energy estimation, which are mandatory for  
216 scientific data processing based on a suitable on-board logic.

#### 217 *3.4. Payload Data Handling Unit*

218 The HERMES Payload Data Handling Unit (PDHU) will be implemented on  
219 iOBC, manufactured by ISIS a commercial on-board computer. This model,  
220 with a weight of  $\sim 100$  g and an average power consumption of 400 mW, will im-  
221 plement all functionalities required for HERMES, such as telecommands (TCs),  
222 housekeeping (HKs), power system commanding (PSU), handling operative  
223 modes of the payload (by TCs or automatically), generating the telemetry pack-  
224 ets (TMs) and managing the interface with the spacecraft. A custom algorithm  
225 making the satellites sensitive X-ray and  $\gamma$ -ray transients, continuously compare  
226 the current data rate of the instrument with the average background data rate  
227 taken previously. When a transient occurs, the events, recorded on a circular  
228 buffer, are then sent to the ground on telemetry packets. Due to the different  
229 families of GRB, ratemeters on different timescales, energy bands and different  
230 geometric regions of the detection plane will be implemented.

## 231 **4. Conclusion**

232 The HERMES project final aim is to realize a new generation instrument  
233 composed by hundreds of detectors onboard nanosatellites. This disruptive tech-

234 nology approach, although based on “underperforming” individual units, allows  
235 to reach overall sensitive areas of the order of  $\sim 1 \text{ m}^2$ , with unprecedented scientific  
236 performance for the study of high-energy transients such as GRBs and gravitational  
237 wave counterparts. The current ongoing phase of the HERMES project  
238 (Technological Pathfinder), focuses on the realization of the three nanosatellites  
239 to be launched in mid-2020, that will demonstrate the proposed approach to  
240 detector design (Silicon Drift Detectors coupled to GAGG:Ce scintillator crystals)  
241 and its performance. In this framework, relevant prototyping activities are  
242 currently under development, towards the implementation phase.

#### 243 **Acknowledgments**

244 HERMES is a *Progetto Premiata MUR*. The authors acknowledge INFN  
245 and FBK (RedSoX2 project and FFK-INFN agreement 2015-03-06), ASI and  
246 INAF (agreements ASI-UNI-Ca 2016-10-U.O and ASI-INAF 2018-10-hh.0).

#### 247 **References**

- 248 [1] R.W. Klebesadel et al., *Astrophysical Journal*, v. 182 (1973) L85
- 249 [2] B.P. Abbott et al., *The Astrophysical Journal Letters*, v. 848 (2017) L12
- 250 [3] M. Marisaldi et al., *Nucl. Instrum. Meth. A*, v. 588 (2008) 37–40
- 251 [4] M. Marisaldi et al., *IEEE Trans. Nucl. Sci.*, v. 51 (2004) 1916
- 252 [5] E. Catt and P. Rehak, *Nucl. Instrum. Meth. in Physics Research*, v. 225  
253 (1984) 600–614
- 254 [6] K. Kawada, et al., *IEEE Trans. Nucl. Sci.*, v. 59, (2012) 2112 – 2115
- 255 [7] M. Sakano, et al., *Journal of Instr.*, v. 9 (2014) P10003
- 256 [8] T. Yanagida, et al., *Optical Materials*, v. 36 (2014) 2016 – 2019
- 257 [9] M. Yoneyama, et al., *Journal of Instr.*, v. 13 (2018) P02023

- 258 [10] M. Ahangarianabhari, et al., Journal of Instr., v. 9 (2014) C03036
- 259 [11] R. Campana, et al., Journal of Instr., v. 9 (2014) P08008

ACCEPTED MANUSCRIPT